FINE STRUCTURE AND ELECTRON CYTOCHEMICAL STUDIES OF *SCLEROTIUM ROLFSII* SACC.

By N. G. Nair,* N. H. White,* D. M. Griffin,* and Suzanne Blair†

[*Manuscript received November* 4, 1968]

Summary

A characteristic feature of the hyphal cells of *S. rolfsii* is an electron-dense sheath surrounding the cell wall. The cell sheath could act as a barrier to diffusion of gases. The septal pore apparatus in *S. rolfsii* conforms to the general pattern of dolipore septum in other basidiomycetes, and appears to be well adapted to protoplasmic streaming and subsequent plugging of the septal pore. A prominent feature of *S. rolfsii* is the presence of concentric and parallel lamellar structures in the hyphal cells. We believe that lomasomes originate through a process of budding of the concentric lamellae into tubular vesicles. Though these lamellar structures resemble bacterial mesosomes, these two organelles do not appear to be homologous structures. Through cytochemical tests we have been able to show that oxidative–reductive events are not located in these lamellae but are integrated in the mitochondria of this fungus. The presence of reduced tellurite in the endoplasm probably indicates that oxidative–reductive events are distributed in the cell.

I. Introduction

During an investigation on the effect of changes in partial pressures of oxygen and carbon dioxide on *Sclerotium rolfsii* Sacc., it was considered appropriate to study the corresponding changes in the fine structure of the fungus. Apart from a single observation on the hyphal septum of an unknown species of *Sclerotium* (Moore and McAlear 1962), there appears to be no information available on the fine structure of any species of this genus. There also appears to be no published record of any electron microscopic studies on the structure of true sclerotia produced by fungi. It was, therefore, necessary to study the morphology of the hyphal cells and sclerotia of *S. rolfsii* at the submicroscopic level before attempting to correlate any changes in the cell organelles with changes in partial pressures of oxygen and carbon dioxide.

Besides describing the salient morphological features, this investigation also includes a cytochemical study of the concentric lamellar structures observed in the hyphae of this fungus. Although similar structures have been observed in other fungi (Blondel and Turian 1960; Hyde and Walkinshaw 1966; Ishihara and Iwaya 1966), considerable uncertainty still exists about their function. Because of the close similarity of the lamellar structures ("fungal mesosomes") to bacterial mesosomes, an investigation was made to determine whether these were homologous structures.

* Department of Agricultural Botany, University of Sydney, N.S.W. 2006.
† Electron Microscrope Unit, University of Sydney, N.S.W. 2006.

II. Materials and Methods

Cultures of *S. rolfsii*, maintained at 25°C on malt–Vegemite–agar medium containing 5·0 g of Vegemite, 50·0 g of malt extract, and 20·0 g of agar per litre of distilled water, were used. The fungus had originally been isolated from cowpeas (*Vigna sinensis*) in Sydney, N.S.W.

(*a*) *Light Microscopy*

Mycelial mats 8 days old and mature sclerotia 18 days old were fixed in formol-acetic-alcohol (commercial formalin–glacial acetic acid–70% ethanol, 5 : 10 : 85 v/v) for 24 hr. The materials were dehydrated through an ethanol series, embedded in paraffin wax, and cut with a rotary microtome at a thickness of 10 μ. The sections were stained with safranin–fast green and safranin–cotton blue.

(*b*) *Electron Microscopy*

Mycelia from cultures 8 days old were teased out, taking care to avoid contamination by agar from the medium, and fixed immediately in fixatives indicated in Table 1. Mature sclerotia were either cut into halves and fixed in the solutions, or cut in a freezing microtome at a thickness of 25 μ prior to fixation. In order to circumvent some of the problems of fixation of the hyphal cells and sclerotia, several fixation schedules employing different fixatives and buffering media were adopted (Table 1). After fixation, the materials were briefly washed and dehydrated in an ethanol series at room temperature. Following dehydration, the materials were infiltrated in a mixture of propylene oxide and Araldite, then in Araldite alone, and finally embedded in Araldite. Ultra-thin sections were cut with an LKB Ultrotome, stained in lead citrate for 10 min, and examined in a Siemens Elmiskop I electron microscope.

(*c*) *Shadow Casting*

Structural details of the network of microfibrils in the hyphal cell walls were studied by preparing "pseudo-" or "pre-shadowed" replicas. Mycelial mat was ground in a tissue homogenizer and subjected to ultrasonic treatment using an MSE ultrasonic disintegrator for 1 min to break the cells. The cell matrix consisting of polysaccharides, hemicellulose, and lipid was then removed by treating the broken cells with boiling 2% H_2SO_4 for 20 min followed by boiling 2% NaOH for a similar duration. The preparations were washed thoroughly in distilled water, sprayed onto nitrocellulose-coated copper grids, shadowed with gold–palladium, coated with carbon, and examined under the electron microscope.

(*d*) *Tellurite Reduction in* S. rolfsii

The electron-scattering property of reduced tellurite has been used in locating respiratory enzymes in many species of bacteria (see van Iterson and Leene 1964*a*, 1964*b*). From the results obtained by previous workers, it appears that tellurite has several advantages over tetrazolium compounds for locating centres of reducing activity. This is particularly so for microorganisms where tellurite can conveniently be added to the culture medium. This advantage, together with the electron-opacity of reduced tellurite (metallic tellurium or tellurium oxide) and its precipitation near to the sites of its reduction, makes tellurite a reliable compound for such investigations. The tetrazolium dyes, on the other hand, are reduced in the cell to the corresponding insoluble formazan (Pearse 1961) which tend to crystallize after deposition; and, therefore, accurate localization of the sites of reduction is not often obtained.

The fungus was grown in half-strength potato–dextrose medium (containing 10% potato extract and 0·75% dextrose) in 150-ml Erlenmeyer flasks for 7 days on a shaker. Potassium tellurite (K_2TeO_3) at concentrations of 0·5, 1·0, and 2·0 g/100 ml was added to the 7-day-old culture and let stand for 24 hr. The mycelium was then fixed in 6·5% glutaraldehyde in cacodylate buffer at pH 7·6 for 4 hr at 4°C followed by post-fixation in 1% osmium tetroxide in veronal acetate buffer at pH 7·6 for 2 hr at 4°C. The fungal cells were also fixed in 6·5% glutaraldehyde alone so that the interference of heavy metals other than tellurium could be avoided.

TABLE 1

COMPARISON OF FIXATION SCHEDULES

No.	Fixative	Buffer	pH	Time (min)	Temp. (°C)	Post-fixation	Buffer	pH	Time (hr)	Temp. (°C)	Results
1	1% $KMnO_4$	Aq. soln.	9·0	45	4	2% uranyl acetate	Aq. soln.	4·4	1	4	Membrane systems of the cell wall preserved. Mitochondria rounded, cristae short and dilated. Mosaic pattern of electron-dense and electron-transparent areas in the nuclei. Nucleoli observed. Endoplasm granular but not homogeneous
2	1% $KMnO_4$	Phosphate	7·6	45	4	Nil	—	—	—	—	Poor fixation. Few cell organelles observed
3	1% $KMnO_4$	Veronal acetate	7·6	45	4	2% uranyl acetate	Veronal acetate	7·6	1	4	Same as 1. Cell organelles slightly more electron-dense than in 1
4	1% $KMnO_4$	Aq. soln.	9·0	5	21	1% OsO_4	Veronal acetate	7·6	4	4	Poor fixation
5	1% $KMnO_4$	Aq. soln.	9·0	20	4	1% OsO_4	Veronal acetate	7·6	4	4	Same as 1. Electron-opacity of cell organelles as in 3
6	1% $KMnO_4$	Aq. soln.	9·0	45	4	1% OsO_4	Veronal acetate	7·6	2	4	Good fixation of cell organelles. Membranes of mitochondria, nuclei, and endoplasmic reticulum better defined than 1, 3, and 5. Striations of cell walls and double membrane structure of plasmalemma observed. Dolipore septa well defined
7	1% $KMnO_4$	Phosphate	7·6	45	4	1% OsO_4	Phosphate	7·6	2	4	Poor fixation
8	1% $KMnO_4$	Veronal acetate	7·6	45	4	1% OsO_4	Veronal acetate	7·6	2	4	Similar to 1, 3, and 5. Preservation of cell organelles not as good as 6
9	2% $KMnO_4$	Aq. soln.	9·2	20	4	2% uranyl acetate	Aq. soln.	4·4	1	4	Poor fixation. Plasmalemma broken and folded. Membranes of mitochondria dilated. Endoplasm as in 1
10	2% $KMnO_4$	Phosphate	7·6	20	4	Nil	—	—	—	—	Poor fixation. Similar to 9
11	2% $KMnO_4$	Veronal acetate	7·6	20	4	2% uranyl acetate	Veronal acetate	7·6	1	4	Moderately well fixed. Organelles less defined than in 1, 3, 5, 6, and 8
12	1% OsO_4	Phosphate	7·6	240	4	Nil	—	—	—	—	Poor fixation of cell organelles
13	1% OsO_4	Veronal acetate	7·6	240	4	Nil	—	—	—	—	Poor fixation. Same as 12
14	6·5% glutaraldehyde	Cacodylate	7·6	240	4	1% OsO_4	Phosphate	7·6	2	4	Poor fixation. Same as 12
15	6·5% glutaraldehyde	Cacodylate	7·6	240	4	1% OsO_4	Veronal acetate	7·6	2	4	Good fixation of cell organelles. Ground substance of endoplasm granular with particles resembling ribosomes. Nucleoli observed. Mitochondria elongated. Cristae long, undilated, and close together. Concentric membrane system and cisternae observed. Structure of cell wall, plasmalemma, and dolipore septum as in 6
16	Aqueous 1% $KMnO_4$ (pH 9, 5–10 min, 4°C), 6·5% glutaraldehyde	Cacodylate	7·6	240	4	1% OsO_4	Veronal acetate	7·6	2	4	Good fixation. Comparatively less defined than 15

III. Observations

(*a*) *Light Microscopy*

The hyphae of *S. rolfsii* are well branched and often grow in the form of strands (*HS*, Fig. 1). Clamp connections are common (*CC*). The hyphae are hyaline, sparsely septate, apparently thin-walled, and measure 3–5 μ in average width. The mature sclerotium (Fig. 2) has an outer zone (*OZ*) of dark brown rind (*R*) consisting of 1–3 layers of thickened cells each measuring about 2–5 μ, a middle zone (*MZ*) of 5–8 compact layers of thickened densely staining cells approximately 16–19 by 9–11 μ, and an inner zone (*IZ*) of loosely arranged normal vegetative hyphae. The inner zone is also characterized by air spaces.

(*b*) *Electron Microscopy*

(i) *Morphology of Hyphae*

The fine structure of *S. rolfsii* resembles that of certain other basidiomycetes although there are conspicuous differences. Those features that are characteristic of *S. rolfsii* are described below.

An electron-dense sheath (*CS*) of 1–3 μ in thickness surrounds the cell wall of hyphae (Figs. 3, 9, 14). It is not clear whether the dense granular particles (*GP*) that aggregate at the periphery of the cell sheath are artifacts (Fig. 3). The shadowing technique has shown that the cell walls possess a cross-fibrillar structure (Fig. 4). The crossed microfibrils show different directions of orientation. Hyphal anastomosis is very commonly observed (Fig. 5).

The hyphae are irregularly partitioned by septa associated with dolipore structure (Figs. 3, 6, and 7). The septum conforms to the structure of dolipore septum described in other basidiomycetes. The mature dolipore septum shows a ring of dense double membrane within the cavity of the pore (Fig. 6). The plug that closes the septal pore in older mycelium appears to be perforated (*PP*) (Fig. 7). The "septal pore cap" or "parenthesome" is porous and lamellar.

The plasmalemma shows a double-membrane structure with two electron-dense layers enclosing an electron-transparent layer. It forms deep invaginations which appear ellipsoidal and circular in cross sections. The endoplasm is granular and the endoplasmic reticulum (*ER*) appears as long agranular double membrane strands. Cisternae (*CIS*) are formed by the endoplasmic reticulum (Fig. 8). The only characteristic feature of the nucleus is the presence of a prominent nucleolus (*NC*) occupying about 15–20% of the nuclear volume (Fig. 9). Mitochondria do not appear to be different in their basic structure from those described in other fungi.

A unique and prominent feature of *S. rolfsii* is the presence of concentric and parallel lamellar structures in the hyphal cells. The lamellae appear as smooth double-membrane structures with two electron-dense layers bounding an electron-transparent layer [Figs. 3 (*CL*) and 10]. The concentric lamellar system may be 5–6-layered (Fig. 10). Rarely some of the layers of the concentric ring appear discontinuous with ends either recurved or rolled inwards. The lamellae possess dilated or club-shaped ends analogous to golgi dictyosomes and appear to bud off tubular vesicles (Fig. 11). This process leads to the formation of lomasome structures which

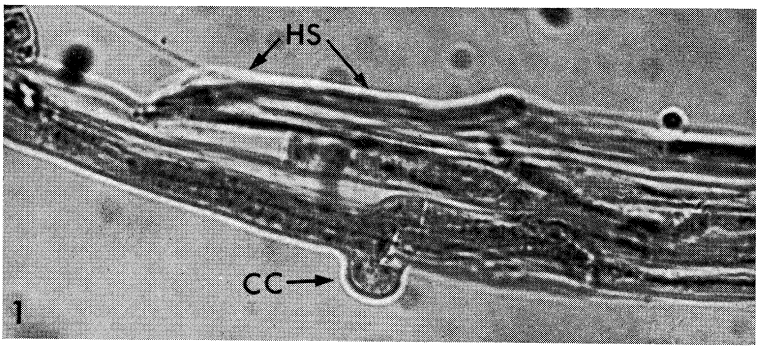

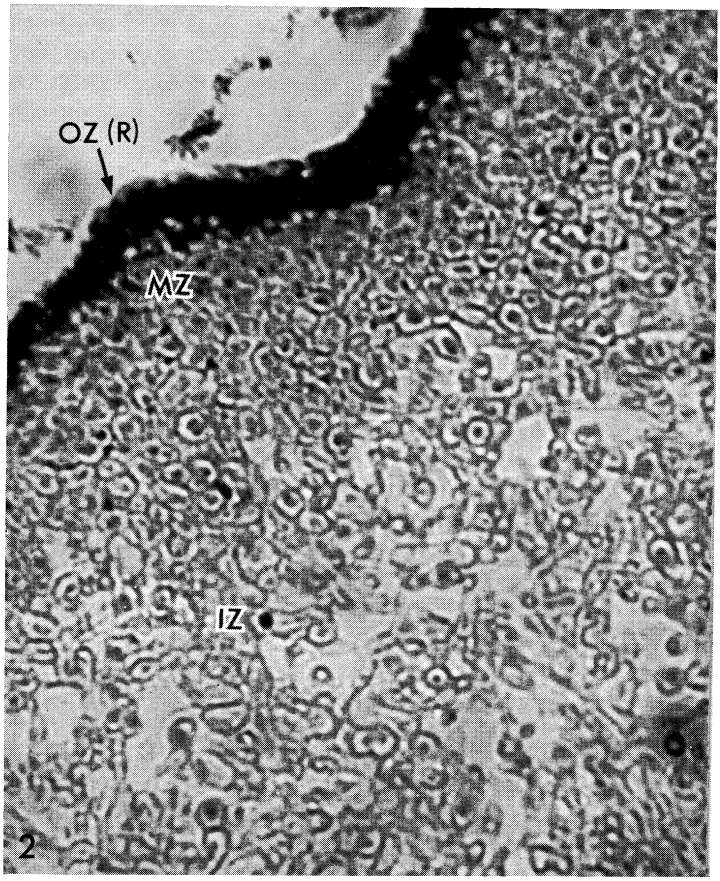

Fig. 1.—Hyphal strand (*HS*) showing clamp connection (*CC*). ×1,250.
Fig. 2.—Transverse section of mature sclerotium. *R*, rind; *OZ*, *MZ*, *IZ*, outer, middle, and inner zone respectively. ×300.

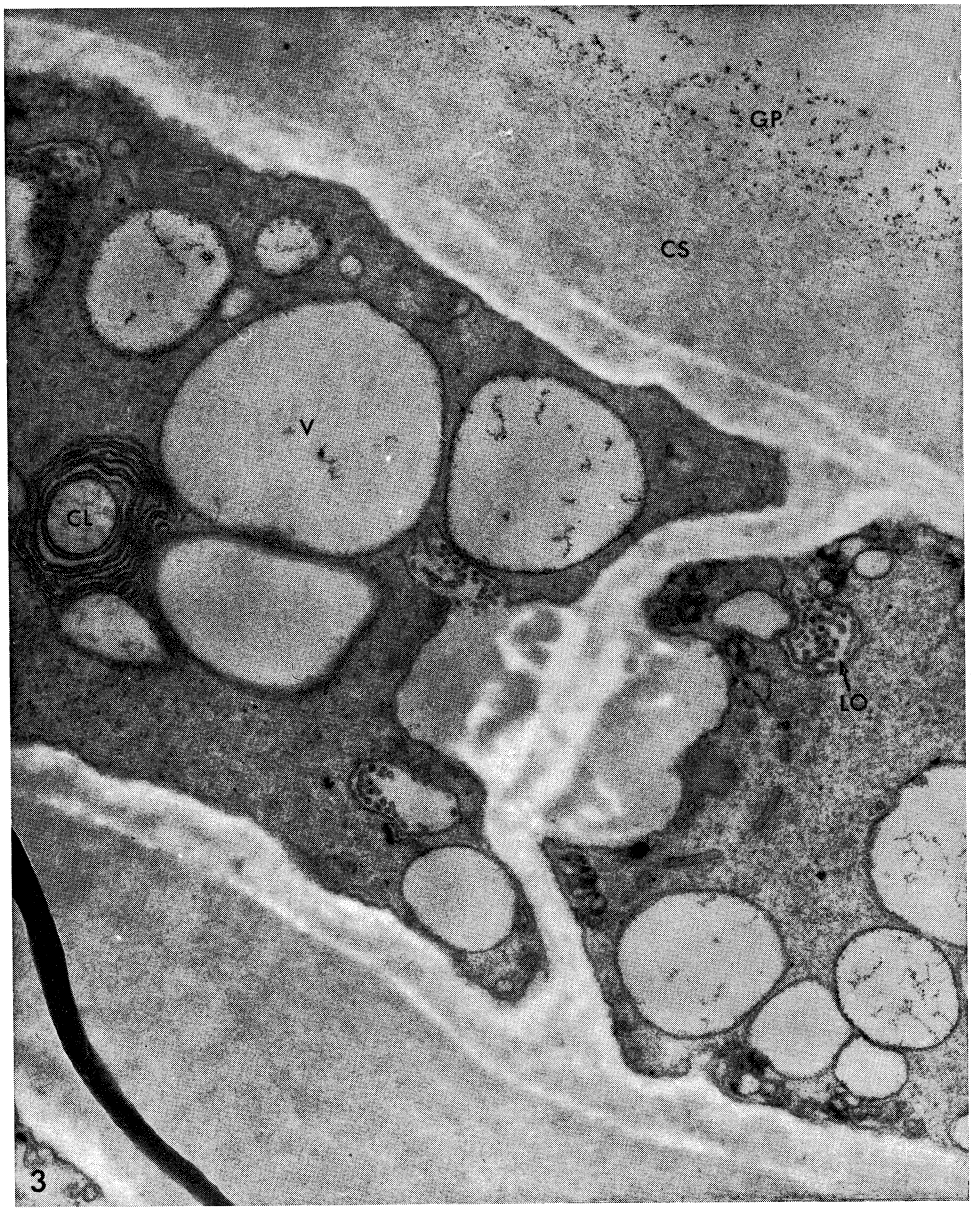

Fig. 3.—Longitudinal section of hypha through dolipore septum. *CL*, concentric lamellae; *CS*, cell sheath; *GP*, granular particles; *LO*, lomasomes; *V*, vacuole. Fixation schedule 15 in Table 1. ×35,000.

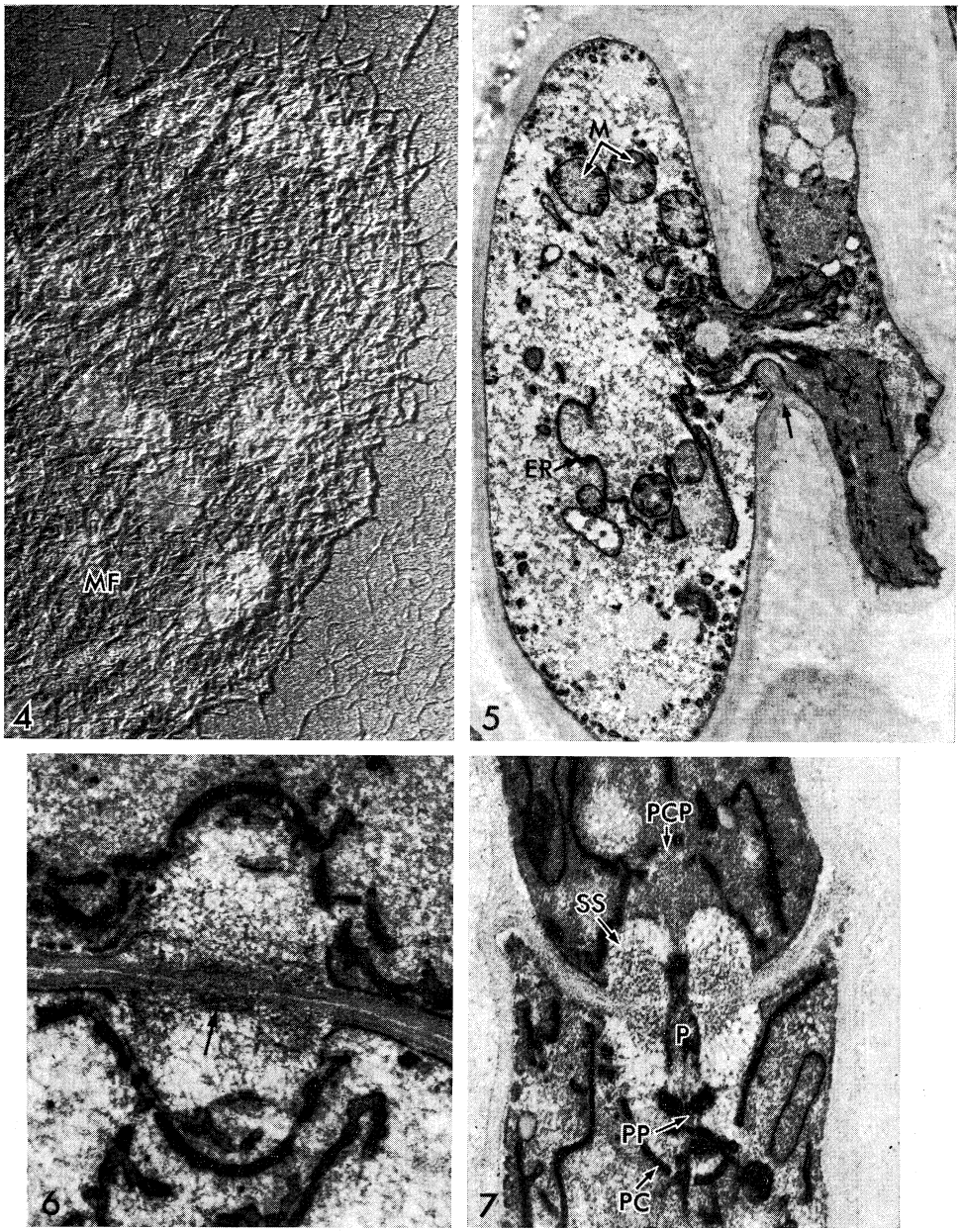

Fig. 4.—Shadowed replica of hyphal cell wall. *MF*, microfibrils. ×25,000.

Fig. 5.—Hyphal anastomosis (arrow). *ER*, endoplasmic reticulum; *M*, mitochondria. Fixation schedule 6 in Table 1. ×7,500.

Fig. 6.—Dolipore septum showing ring of double membrane (arrow). Fixation schedule 5 in Table 1. ×29,000.

Fig. 7.—Dolipore septum; pore plug. *P*, septal pore; *PC*, pore cap; *PP*, pore plug; *PCP*, pore-cap pores; *SS*, septal swelling. Fixation schedule 16 in Table 1. ×23,200.

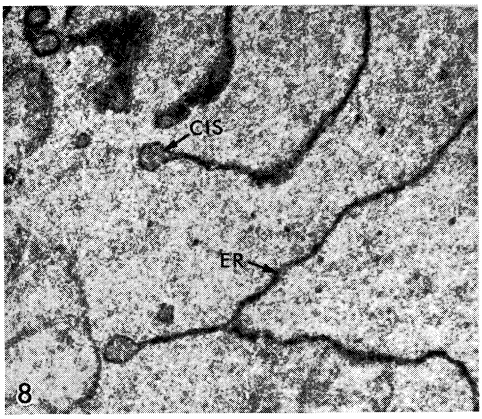

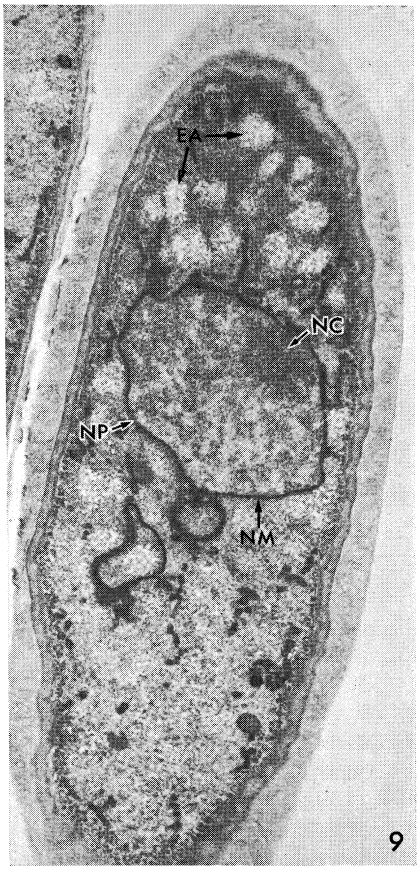

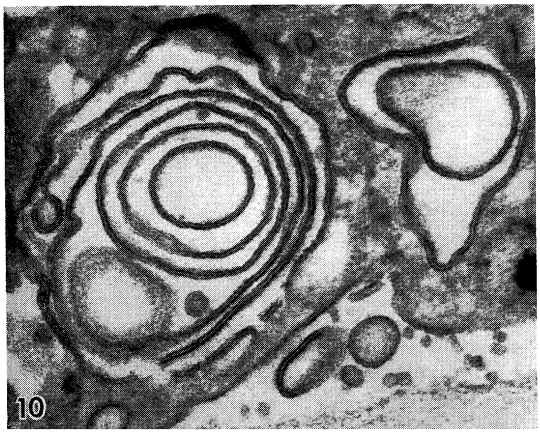

Fig. 8.—Portion of hypha showing cisternae (*CIS*) formed by endoplasmic reticulum (*ER*). Fixation schedule 3 in Table 1. ×23,500.

Fig. 9.—Transverse section of hypha showing details of nucleus. *EA*, electron-transparent areas; *NC*, nucleolus; *NM*, nuclear membrane; *NP*, nuclear pore. Fixation schedule 3 in Table 1. ×14,000.

Fig. 10.—System of concentric membranes showing recurved ends. Fixation schedule 15 in Table 1. ×80,000.

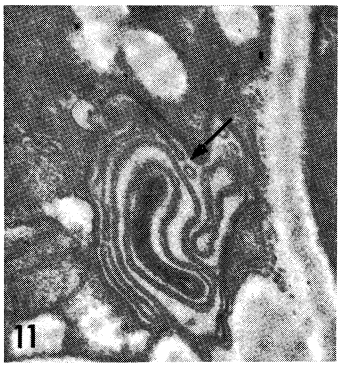

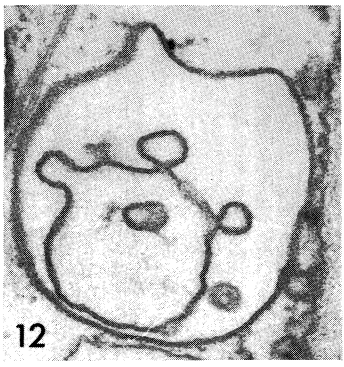

Fig. 11.—System of parallel membranes. Arrow points to the vesicles being cut off by the membranes. Fixation schedule 15 in Table 1. ×30,000.

Fig. 12.—Circular cisternae with budding vesicles. Fixation schedule 15 in Table 1. ×45,500.

are morphologically distinguished by a circular double-membranous envelope enclosing small tubular vesicles. They are extruded to an extra-endoplasmic environment by invagination of the plasmalemma both at the lateral and cross walls (Figs. 3 and 13).

Another characteristic feature of *S. rolfsii* is the presence of vesicles and cisternae scattered throughout the endoplasm (Figs. 12 and 13). Several dense double-membrane structures appear in the ground substance of the endoplasm, and appear to form cisternae. They consist of an external limiting double membrane enclosing 2–4 circular vesicles, either in concentric arrangement or in random distribution. The inner layers of such a system of cisternae cut off round vesicles by means of budding. The size of these vesicles ranges from $0 \cdot 2$ to $1 \cdot 0$ μ in diameter. In one instance, all the stages in the process of budding appear in the same cisterna (Fig. 12). Frequently the membranes of the cisternae have a diffuse appearance, presumably due to oblique sectioning. The cisternae with the inner vesicles are sometimes associated with vacuoles (*V*, Fig. 13). Though the cisternae are formed at any point in the cell, they appear to migrate to the periphery either independently or along with a vacuole. After reaching the lateral wall they seem to pass out of the endoplasm either by a process of invagination of the plasmalemma (as in the case of lomasomes) or by the dissolution of its membrane and that of the plasmalemma at their point of contact.

(ii) *Morphology of Sclerotia*

Though good fixation of the cell organelles was not obtained, the pattern of cellular arrangement in the sclerotia was observed. The early stages in the development of sclerotia were characterized by the development of hyphal strands wherein the individual hyphae are interconnected by means of the cell sheath (Fig. 14). Cell walls of the middle zone in a mature sclerotium could be observed, but those of the outer zone (rind) were not fixed well. The cell walls were very thick and showed striations of dense and light layers which followed the contour of the plasmalemma (Fig. 15).

(*c*) *Tellurite Reduction in* S. rolfsii

Following the introduction of the colourless potassium tellurite solution, the cultures of *S. rolfsii* gradually turned grey and finally greyish black. The speed of this colour change increased with increase in concentration of potassium tellurite in the culture medium. No change in colour was observed in the untreated controls. The plasmalemma in the tellurite-treated cells did not show any increase in electron density compared to that of the untreated cells (Fig. 16). The cells that were fixed in glutaraldehyde alone showed deposition of tellurium crystals irregularly in the endoplasm (Fig. 17). Though the structural details of the cell organelles were not clearly seen in these cells, omission of osmium tetroxide as a post-fixative conclusively proved that the deposits in the cells were not artifacts but reduced tellurite itself.

The deposits of reduced tellurite are localized in the mitochondria in the form of black, pin-head deposits (Fig. 16). Relatively larger needle- or rod-shaped crystals, representing the end products of a positive reaction, are also distributed in the general endoplasm. Intracellular deposits of the reaction product were not seen in or on the concentric lamellar structures. Large, dark droplets, probably representing lipids, were observed in the tellurite-treated cells (Fig. 16).

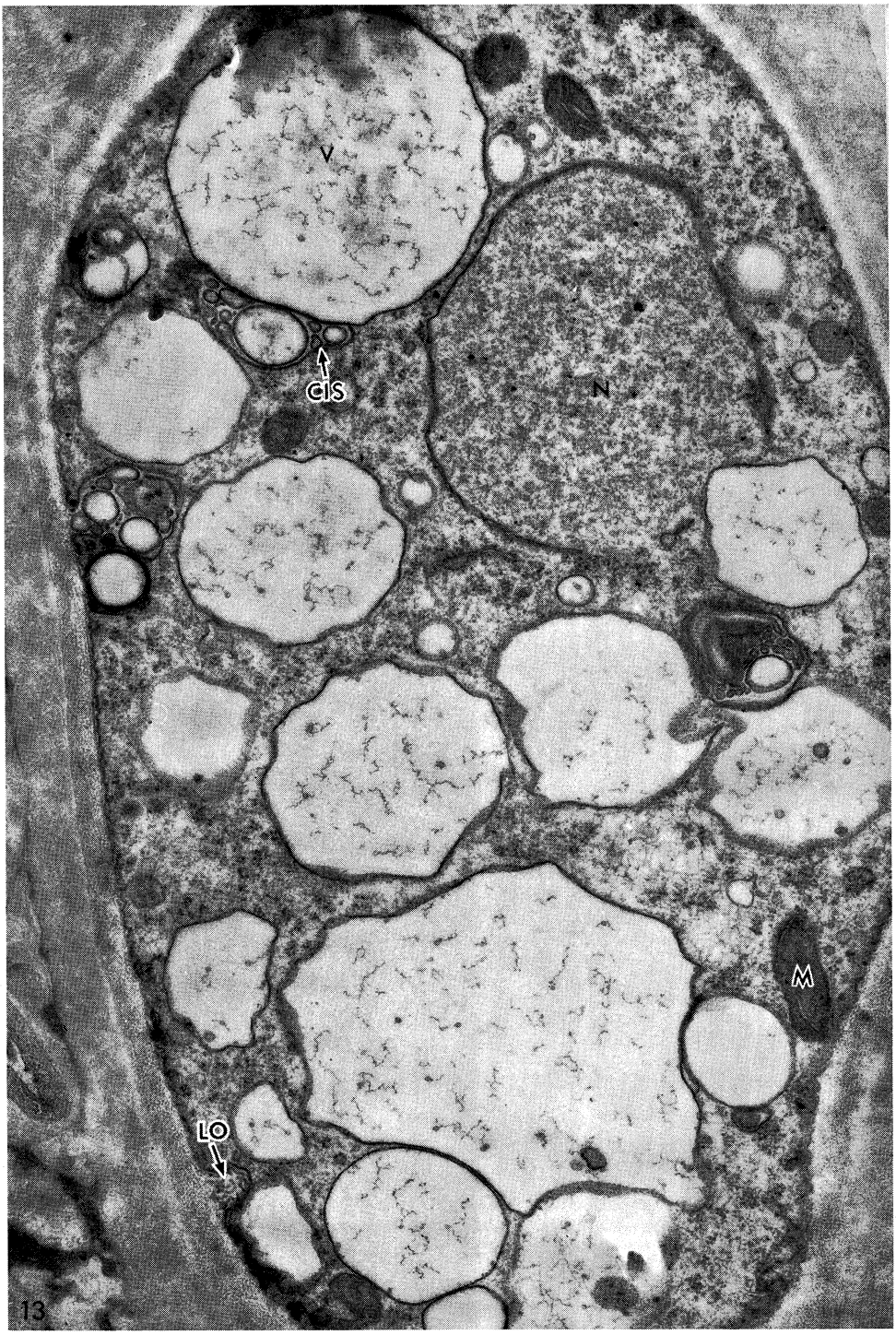

Fig. 13.—Transverse section of hypha showing circular vesicles attached to vacuole (*V*). *CIS*, cisternae; *LO*, lomasomes; *N*, nucleus. Fixation schedule 15 in Table 1. ×23,500.

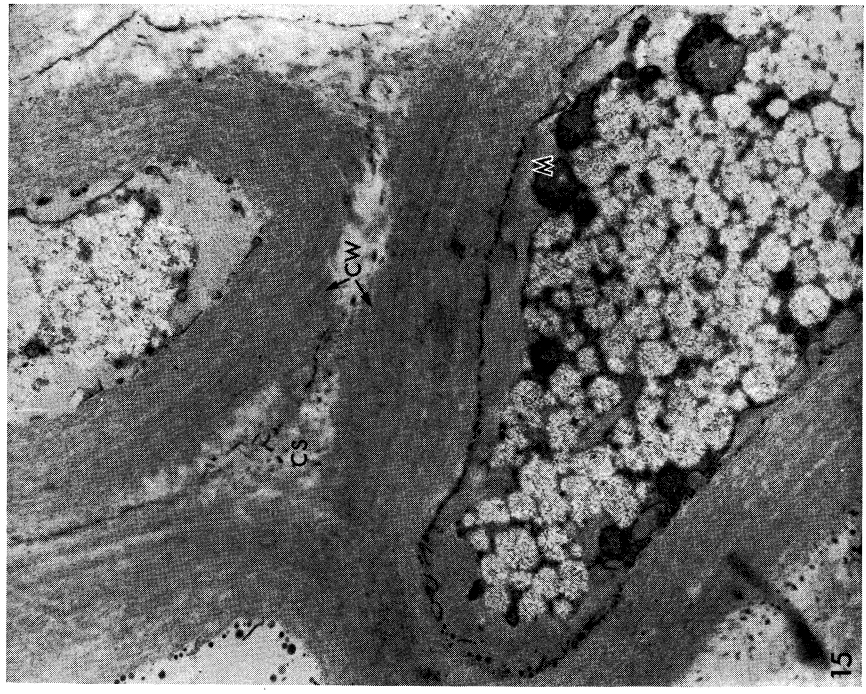

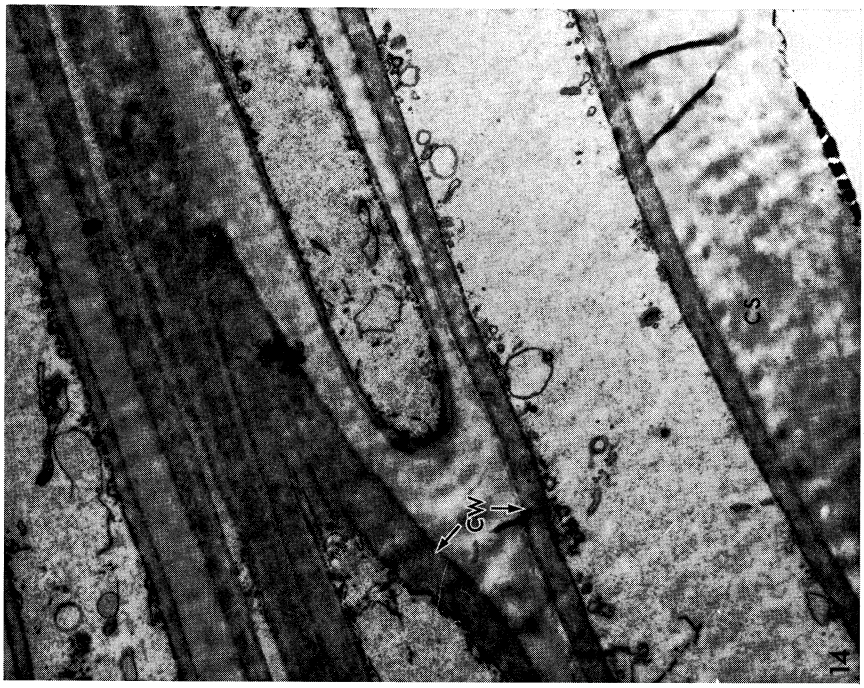

Fig. 14.—Longitudinal section of hyphal strand during early stages in the development of sclerotium. *CS*, cell sheath; *CW*, cell wall. Fixation schedule 6 in Table 1. ×7,500.

Fig. 15.—Transverse section through middle zone of sclerotium. *CS*, cell sheath; *CW*, cell wall; *M*, mitochondria. Fixation schedule 6 in Table 1. ×9,900.

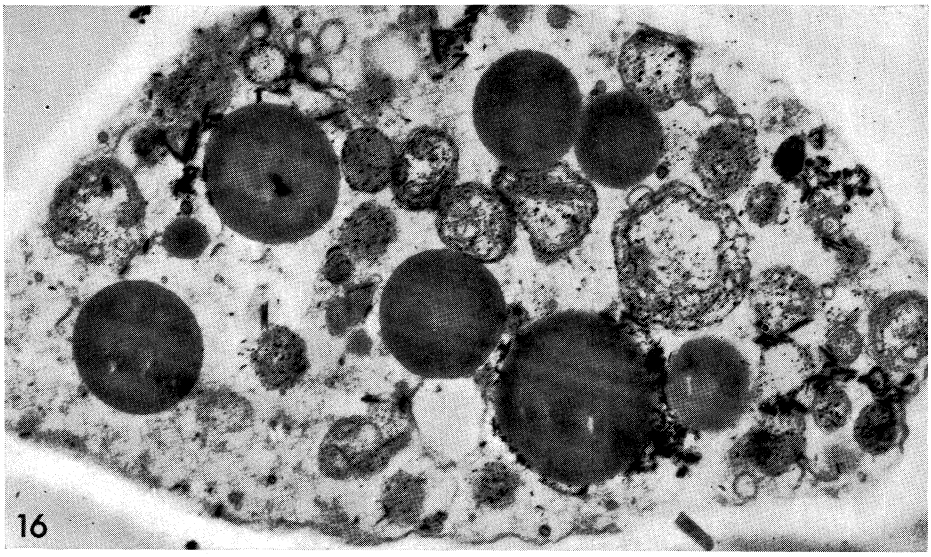

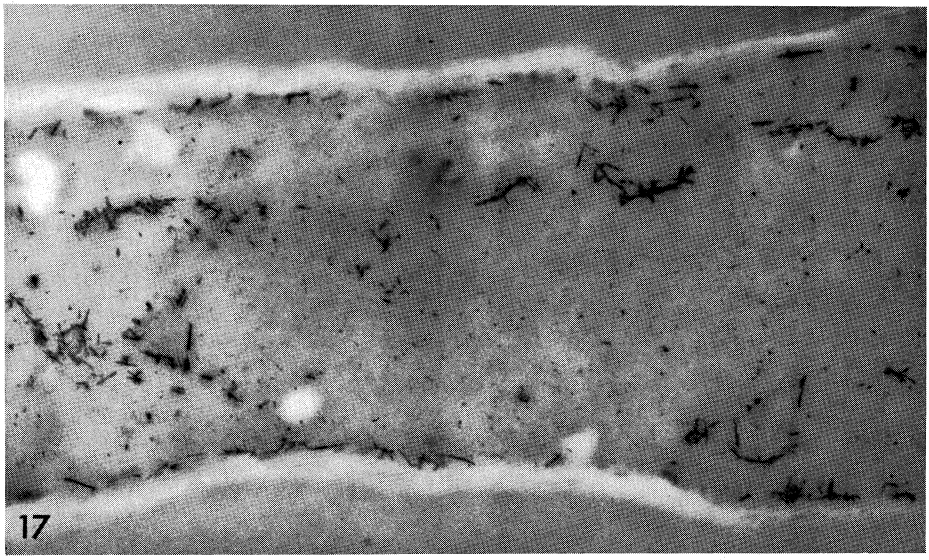

Fig. 16.—Transverse section of hypha showing localization of reduced tellurite in mitochondria and endoplasm. Dark circular bodies appear to be lipids. Fixation schedule 15 in Table 1. $\times 20{,}000$.

Fig. 17.—Longitudinal section of hypha showing deposition of reduced tellurite. Hypha fixed in 6·5% glutaraldehyde in cacodylate buffer at pH 7·6 for 4 hr at 4°C. $\times 20{,}500$.

IV. Discussion

A characteristic feature of the hyphal cells of *S. rolfsii* is an electron-dense sheath surrounding the cell wall. The cell sheath appears to be initially hydrophobic because the mycelium is difficult to wet and only shaking in water can wet the hyphae. Griffin and Nair (1968) showed that although mycelial growth of *S. rolfsii* occurred equally well at oxygen concentrations of 4–21%, sclerotia were not formed at concentrations between 0·2 and 13·3% even at the end of 19 days. These results probably indicate that the cell sheath observed in the present work could act as a barrier to diffusion of gases.

The septum of *S. rolfsii* conforms to the general pattern of dolipore septum described in other basidiomycetes (Girbardt 1958, 1961; Moore and McAlear 1962; Wells 1964; Wilsenach and Kessel 1965), particularly *Rhizoctonia solani* (Bracker and Butler 1962, 1963). A ring of dense double membrane seen within the cavity of the septal pore probably initiates the formation of the plug that closes the pore. The significance of the perforation in the plug is not known. From the electron micrographs of the septal pore apparatus in *S. rolfsii* and *R. solani* it is evident that both the species are well adapted for protoplasmic streaming and subsequent plugging of the septal pore. Bracker and Butler (1963, 1964) have shown that mitochondria migrate through the septal pore in *R. solani*. Organelles resembling mitochondria have also been observed by us to lie within the septal pore cap pores in *S. rolfsii*. What is interesting from a biochemical point of view is the possibility that active migration of mitochondria from cell to cell might influence the respiratory processes of the fungus. We have shown in the present investigation that the respiratory enzyme systems are integrated in the mitochondria. This becomes more significant when we know that the septal pore is closed by a plug in older cells where bioenergetic processes are supposedly slow.

We have not observed nuclei within the septal pore in any of our electron micrographs. However, in our opinion this does not preclude the possibility of nuclear migration from cell to cell which may occur either through clamp connections frequently seen in young and old hyphae or through anastomosing hyphae. In fact, if the septal pore becomes closed in old hyphae, nuclear migration could be expected to occur through the clamp connections or hyphal anastomoses.

A prominent feature of *S. rolfsii* is the presence of concentric and parallel lamellar structures in the hyphal cells. Although the lamellae possess dilated or club-shaped ends evidence is lacking to designate these structures as true golgi apparatus. They may, however, be considered as a primitive type of golgi apparatus. We believe that lomasomes in *S. rolfsii* originate through a process of budding of the concentric lamellae into tubular vesicles. This was further confirmed by demonstrating that these lamellae or mesosome-like structures did not serve as sites of oxidative–reductive events. The results obtained by using potassium tellurite probably indicate that the "fungal mesosomes" or mesosome-like structures described in *S. rolfsii* and other fungi like *Allomyces macrogynous* (Blondel and Turian 1960), *Microsporum gypseum* (Ishihara and Iwaya 1966), and *Lenzites saepiaria* (Hyde and Walkinshaw 1966) are not homologous with bacterial mesosomes, but serve other functions such as formation of lomasomes as in *S. rolfsii* or may even be products of metabolism as in *Allomyces macrogynous* (Blondel and Turian 1960).

Since the intracellular deposits of reduced tellurite are prominently localized in the mitochondria, we assume that the mitochondria form the major sites of reducing activity in *S. rolfsii*. The presence of reduced crystals in the endoplasm probably indicate that oxidative–reductive events are distributed in the cell.

V. Acknowledgments

We thank Miss Robin Arnold for technical assistance. The award of a Sydney University Post-Doctoral Fellowship to one of us (N.G.N.) is gratefully acknowledged.

VI. References

Blondel, B., and Turian, G. (1960).—Relation between basophilia and fine structure of cytoplasm in the fungus *Allomyces macrogynous* Em. *J. biophys. biochem. Cytol.* **7**, 127.

Bracker, C. E., and Butler, E. E. (1962).—Ultrastructure of septal pore apparatus of *Rhizoctonia solani*. Proc. 5th Int. Conf. Electron Microsc., Philadelphia, 1962. Vol. II. p. UU-6.

Bracker, C. E., and Butler, E. E. (1963).—The ultrastructure and development of septa in hyphae of *Rhizoctonia solani*. *Mycologia* **55**, 35–58.

Bracker, C. E., and Butler, E. E. (1964).—Function of the septal pore apparatus in *Rhizoctonia solani* during protoplasmic streaming. *J. Cell Biol.* **21**, 152–7.

Girbardt, M. (1958).—Uber die substruktur von *Polystictus versicolor* L. *Arch. Mikrobiol.* **28**, 255–59.

Girbardt, M. (1961).—Licht- und electrone mikroscopische Untersuchungen an *Polystictus versicolor*. II. Die Feinstruktur von Grundplasma und Mitochondrien. *Arch. Mikrobiol.* **39**, 351–9.

Griffin, D. M., and Nair, N. G. (1968).—Growth of *Sclerotium rolfsii* at different concentrations of oxygen and carbon dioxide. *J. exp. Bot.* **19**, 812–16.

Griffin, D. M., Nair, N. G., Baxter, R. I., and Smiles, D. E. (1967).—Control of gaseous environment of organisms using a diffusion column technique. *J. exp. Bot.* **56**, 518–25.

Hyde, J. M., and Walkinshaw, C. H. (1966).—Ultrastructure of basidiospores and mycelium of *Lenzites saepiaria*. *J. Bact.* **92**, 1218–27.

Ishihara, K., and Iwaya, T. (1966).—Ultrastructure and electron cytochemical studies of *Microsporum gypseum*. Proc. 6th Int. Conf. Electron Microsc., Kyoto, 1966. Vol. II. p. 107.

Iterson, W. van, and Leene, W. (1964*a*).—A cytochemical localization of reductive sites in a Gram-positive bacterium. Tellurite reduction in *Bacillus subtilis*. *J. Cell Biol.* **20**, 361–75.

Iterson, W. van, and Leene, W. (1964*b*).—A cytochemical localization of reductive sites in a Gram-negative bacterium. Tellurite reduction in *Proteus vulgaris*. *J. Cell Biol.* **20**, 377–87.

Moore, R. T., and McAlear, J. H. (1962).—Fine structure of Mycota. 7. Observations of septa of ascomycetes and basidiomycetes. *Am. J. Bot.* **49**, 86–94.

Pearse, A. G. E. (1961).—"Histochemistry." 2nd Ed. (J. & A. Churchill: London.)

Wells, K. (1964).—The basidia of *Exidia nucleata*. I. Ultrasturcture. *Mycologia* **56**, 326–41.

Wilsenach, R., and Kessel, M. (1965).—On the function and structure of septal pore of *Polyporus rugulosus*. *J. gen. Microbiol.* **40**, 397–400.